

MATHEMATICAL MODEL

Luminal chloride concentration in i -th TAL, $i = 1, 2$:

$$\frac{\partial C_i}{\partial t}(x, t) = -F_i(C_{MD_i}(t)) \frac{\partial C_i}{\partial x}(x, t) - \frac{V_{max} C_i(x, t)}{K_M + C_i(x, t)} - P(C_i(x, t) - C_e(x))$$

TAL flow, feedback + coupling + perturbations:

$$F_i(C_{MD_i}(t)) = 1 + K_1 \tanh(K_{2i}(C_{opi} - C_{MD_i}(t))) + \sum_j \phi_{ij}(F_i - F_j) + \text{Perturbations}$$

Delay of signal across JGA:

$$C_{MD_i}(t) = \int_{-\infty}^t \psi_{\delta}(t - s - \delta/2) C_i(1, s - \tau_{pi}) ds$$

All variables and parameters have been nondimensionalized. The space variable x is oriented so that it extends from the entrance of the TAL ($x = 0$), through the outer medulla, and into the cortex to the site of the MD ($x = 1$).

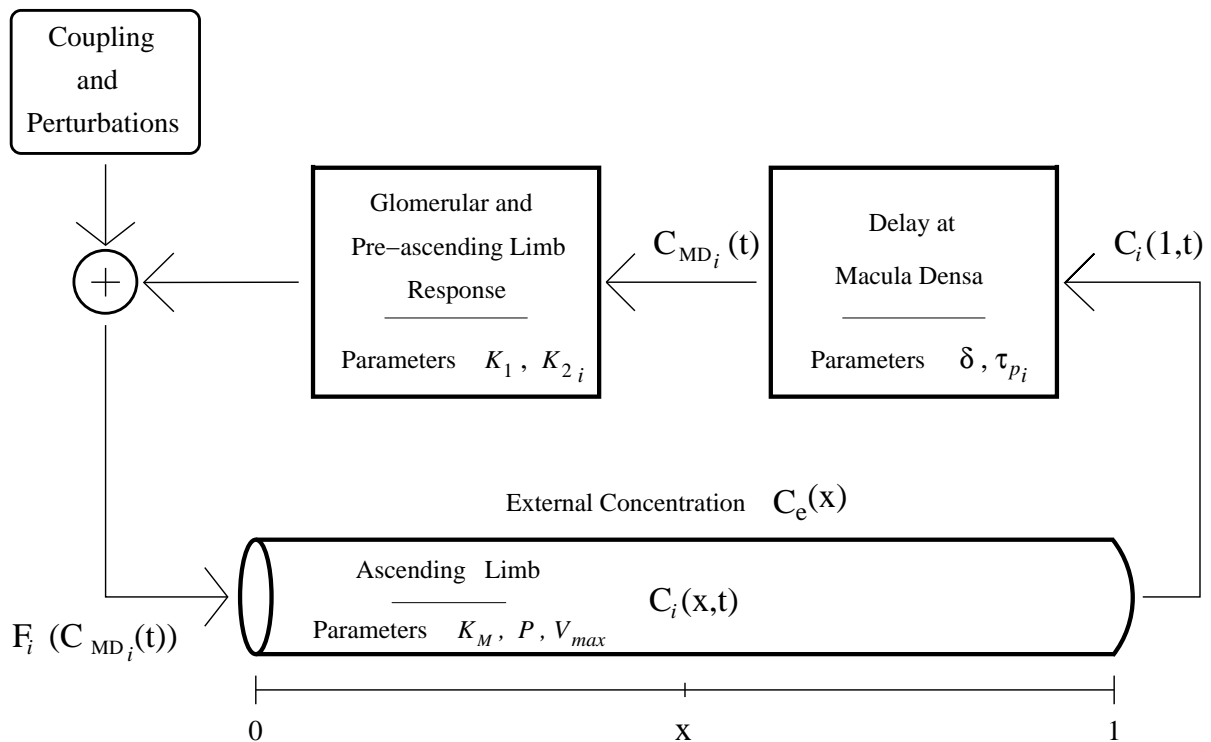


Figure M1. Schematic of model components.

Characteristic Equation

$$1 = \gamma e^{-\lambda(\tau_{pi} + \delta/2)} \left(\int_0^1 e^{-\frac{\lambda(1-x)}{\zeta}} \exp \left(-P \int_x^1 \frac{C'_e(y)}{S'_i(y)} dy \right) dx \right) \left(\int_{-\delta/2}^{\delta/2} \psi_\delta(y) e^{-\lambda y} dy \right)$$

$$\text{where } \psi_\delta(u) = \begin{cases} (1 + \cos(2\pi u/\delta))/\delta, & -\delta/2 \leq u \leq \delta/2 \\ 0, & |u| > \delta/2 \end{cases}$$

The parameter ζ provides TAL volume scaling relative to the base case of $\zeta = 1$.

Solutions of the characteristic equation must be approximated numerically.

Base-Case Parameter Values

Parameter	Dimensional Value
C_o	275 mM
C_{op}	31.96 mM
K_M	70.0 mM
L	0.500 cm
P	1.50×10^{-5} cm/s
Q_{op}	30.0 nl/min
ΔQ	18.0 nl/min
r	10.0 μm
T	15.708 s
V_{max}	$14.5 \text{ nmole} \cdot \text{cm}^{-2} \cdot \text{s}^{-1}$
α	0.200 (dimensionless)
δ	3.00 s
τ_{pi}	2.00 s

Glossary

Parameters

C_o	[Cl ⁻] at TAL entrance (mM)
C_{op}	steady-state [Cl ⁻] at MD (mM)
k	sensitivity of TGF response (l/mM)
K_M	Michaelis constant (mM)
L	length of TAL (cm)
P	TAL chloride permeability (cm/s)
Q_{op}	steady-state SNGFR (nl/min)
ΔQ	TGF-mediated range of SNGFR (nl/min)
r	luminal radius of TAL (μm)
T	steady-state TAL transit time (s)
V_{max}	maximum transport rate of chloride ($\text{nmole}\cdot\text{cm}^{-2}\cdot\text{s}^{-1}$)
K_1	$\Delta Q/2Q_{op}$
K_2	$kC_o/2$
ϕ_{ij}	coupling parameter between TALs i and j
α	fraction of SNGFR reaching TAL
δ	distributed delay interval at the JGA (s)
γ	feedback gain magnitude, $-K_1K_2S'(1)$
τ_{pi}	pure delay interval at the JGA (s)
D	effective delay interval ($\tau_p + \delta/2$) at the JGA (s)
ζ	TAL volume scaling

Independent Variables

t	time (s)
x	axial position along TAL (cm)

Specified Functions

$C_e(x)$	extratubular [Cl ⁻] (mM)
$\psi_\delta(t)$	function for distributed delay

Dependent Variables

$C(x, t)$	TAL [Cl ⁻] (mM)
$C_{MD}(t)$	effective MD [Cl ⁻] (mM)
$F(C_{MD}(t))$	TAL fluid flow (nl/min)
$S(x)$	steady-state TAL [Cl ⁻] (mM)

INTRODUCTION

The tubuloglomerular (TGF) system is a key regulator of SNGFR and of water and electrolyte delivery to the distal nephron. In the 1980's, experiments in rats by Leyssac and colleagues demonstrated that nephron flow and related variables may exhibit regular oscillations with a period of ~ 30 s [8] (Fig. 1, panel A). Mathematical models have indicated that these regular oscillations are TGF-mediated and that they arise from a bifurcation: if feedback-loop gain is sufficiently large, and if the delay in TGF signal transmission at the juxtaglomerular apparatus (JGA) is sufficiently long, then the stable state of the system is a regular oscillation and not a time-independent steady state [5, 7].

In addition, experiments have shown that the TGF system in hypertensive rats may exhibit irregular oscillations [4, 9], (Fig. 1, panels B and C). These oscillations appear to have characteristics of deterministic chaos [9]. Mathematical models that represent spatially-distributed NaCl transport along the TAL have not predicted the irregular oscillations [5, 7], although some models that use a less realistic TAL model have exhibited such oscillations [1].

The studies summarized here show that two coupled model nephrons (i.e., nephrons that have the capability to influence each other's glomerular filtration rate) can exhibit a variety of complex dynamic behaviors. In particular, irregular, mixed-mode oscillations resembling those reported in [9] may arise from the coupling of nephrons with sufficiently different bifurcation parameters.

Oscillations in Proximal Tubule Pressure Recorded by Yip et al. and Corresponding Power Spectra

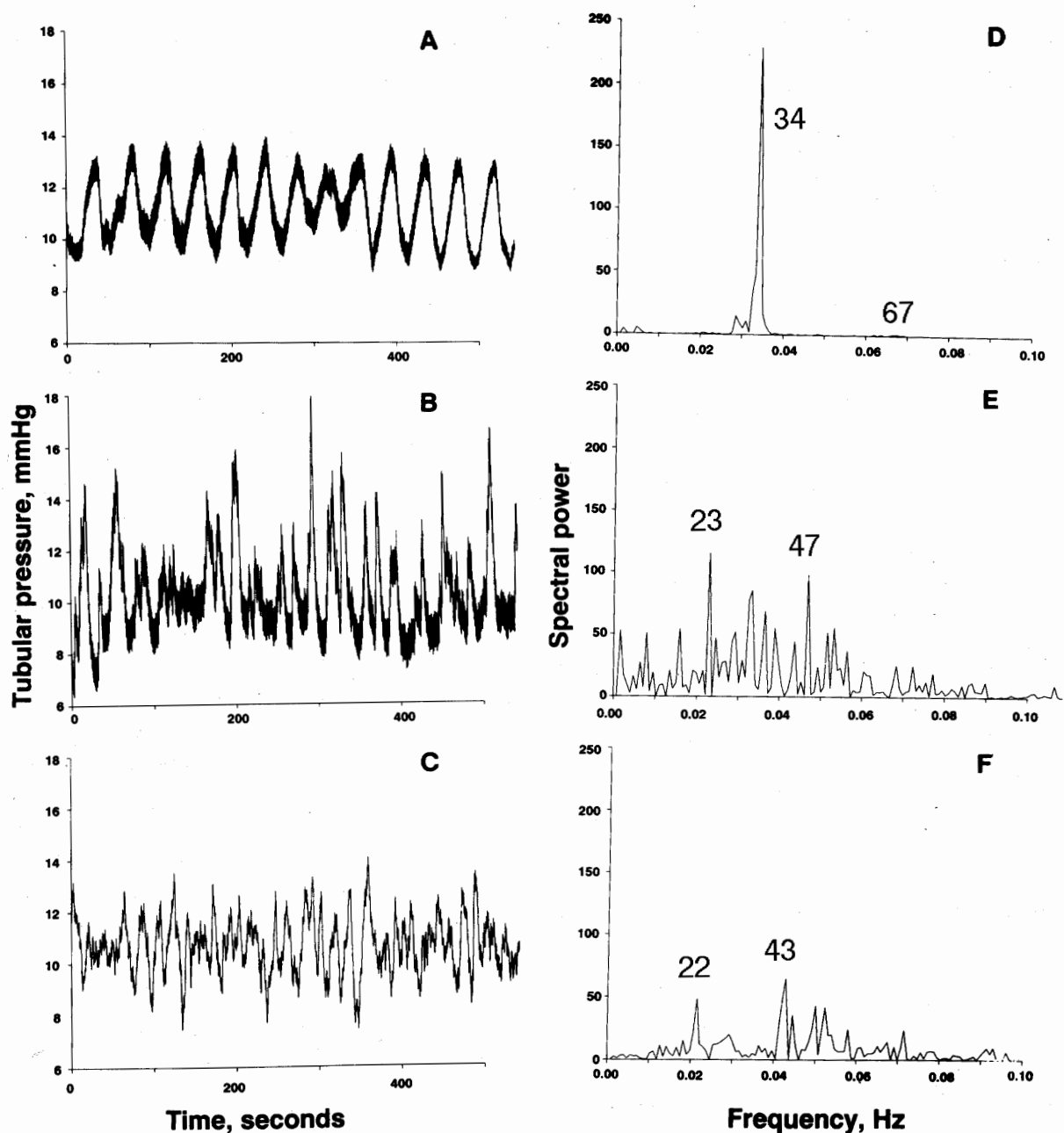


FIGURE 1. Oscillations in proximal tubule pressure measured by Yip and collaborators [9], and corresponding power spectra. Panel A, normal Sprague-Dawley rat; panel B, spontaneously hypertensive rat; panel C, 2-kidney, 1-clip Goldblatt hypertensive rat. Corresponding power spectra are given in panels D, E, and F. We have labeled the dominant peaks in the power spectra with their frequencies (in mHz).

A “DOUBLED-FREQUENCY” PARAMETER REGIME

Our previous modeling studies have indicated that two dimensionless parameters, γ and τ , play a key role in determining the stable state of the TGF system [7]. The feedback-loop gain γ is the product of two factors: (1) the slope of the TGF response curve, and (2) the magnitude of the luminal $[\text{Cl}^-]$ profile alongside the macula densa. The delay parameter τ is the ratio of two delays: $\tau = D/T$, where D is the delay in TGF signal transmission across the JGA and T is the steady-state transit time of fluid through the TAL.

Analysis of the model leads to a characteristic equation, which predicts stable and oscillatory solutions in different parameter regimes. A resulting bifurcation diagram for a hypertensive rat is given in Fig. 2. This diagram assumes increased TAL volume (or increased TAL transit time) for hypertensive rats relative to normotensive rats (*vide infra*), based on the frequency shift observable in Fig. 1.

Below the curves in Fig. 2, the model solution is a stable time-independent steady state. In the region “Stable 1- f LCO,” the stable solution is oscillatory at a fundamental frequency f_1 . In region “Stable 2- f LCO,” analysis and simulations indicate that the stable solution is oscillatory with frequency $f_2 \approx 2f_1$.

In Fig. 3, we exhibit model-generated oscillations in SNGFR (left column) and corresponding power spectra (right column) using parameters corresponding to $\tau_p = 3.5$ and gains

A: $\gamma = 4.5$ **B:** $\gamma = 5.5$, and **C:** $\gamma = 6.5$.

Point **A**, below the curves, corresponds to a stable time-independent steady state: a perturbed solution will always return to that steady state. Point **B**, in the region “Stable $1-f$ LCO,” corresponds to a stable oscillatory solution; for this point, the fundamental frequency is $f_1 = 34$ mHz. Point **C**, in the region “Stable $2-f$ LCO,” corresponds to a “doubled-frequency” stable oscillatory solution; for this point, the fundamental frequency is $f_2 = 66$ mHz, which is $\approx 2f_1$.

IRREGULAR OSCILLATIONS IN COUPLED NEPHRONS

Much experimental evidence indicates that nephrons having afferent arterioles arising from the same cortical radial artery can exhibit coupled oscillations [2, 6]. In Figs. 4 and 5 we examine the effect of coupling between a model nephron in the double-frequency regime and model nephrons that have nearby parameters. Figure 4, which shows the same bifurcation relationships as Fig. 2, contains labeled Points **X**, **a**, **b**, and **c**. For the nephron marked by Point **X**, and coupled with Point **a**, **b**, or **c**, Fig. 5 exhibits typical model solutions for SNGFR and corresponding power spectra; the Panels a1 and a2 correspond to Point **X** coupled with Point **a**; the analogous convention holds for Points **b** and **c**. The most irregular pattern was obtained for **X** when it was coupled with **b**, which had the most differing parameters. In this case, the frequencies of 35 and 67 mHz were most excited.

It may be noteworthy that when nephrons are coupled, the model system exhibits two differing, but nearby, frequencies, rather than merely a single $1-f$ or $2-f$ frequency; these “doublet” frequencies, which can sometimes be observed in power spectra at both the $1-f$ and $2-f$ regimes, correspond to eigenvalue pairs that emerge in the coupled system.

POTENTIAL RELEVANCE TO HYPERTENSION

Published power spectra for hypertensive rats (Fig. 1, panels E and F) exhibit two prominent characteristics: (1) each spectrum has two dominant peaks, with the second peak at a frequency that is about twice that of the first; and (2) the apparent fundamental frequency (~ 23 mHz) is reduced substantially relative to a normotensive animal (~ 34 mHz).

We believe that the reduced fundamental frequency, relative to normotensive rats, arises from greater TAL volume (or, greater transit time), which would reduce the dimensionless parameter τ . Moreover, hypertensive rats have been found to have elevated gains, sometimes measured as high as 9.9 [3]. Thus the gray disk in Figs. 3 and 4 may approximate the hypertensive rat parameter regime.

It may be noteworthy that Holstein-Rathlou and Leyssac found no regular oscillations in spontaneously hypertensive rats; rather they found either a steady-state or irregular oscillations [4]. This suggests that either a nephron, or groups of nephrons were in the stable steady-state regime,

or that one or more nephrons were in the $2-f$ regime—but that no single, uncoupled nephron was in the $1-f$ regime.

We hypothesize that the two dominant peaks in power spectra from hypertensive rats arise from coupling between nephrons of differing fundamental frequency, as exhibited in the model simulations in Fig. 5. The simulations indicate that the coupling may result in mixed-mode oscillations in which both the $1-f$ and $2-f$ oscillations are excited.

Irregularity in the model waveforms arises in part from the only approximate doubling of frequency. A degree of complexity in the model power spectra arises from the emergence of doublet frequencies; close examination of Fig. 1, panels E and F, suggests that such doublets may be present *in vivo*.

More generally, based on the considerations above, we hypothesize that the irregular oscillations observed in the hypertensive rats [9] arise, at least in part, from internephron coupling between two or more nephrons, with at least one of them having parameters in the $2-f$ regime.

However, this model study appears to provide no explanation for those distinct frequencies in the experimental power spectra that cannot be attributed to $1-f$ or $2-f$ oscillations or their respective doublets. A more inclusive model formulation will likely be required to investigate the origin of those other frequencies.

SUMMARY

1. We have used a simple mathematical model of the tubuloglomerular feedback loop to investigate how oscillatory states may depend on physiologic parameters and nephron-to-nephron coupling through the afferent arteriolar response.
2. The physiologic parameter space has regions that correspond to three qualitatively different model behaviors:
 - a time-independent steady state,
 - a sustained oscillation with frequency f , and
 - a sustained oscillation with frequency $\sim 2f$.
3. The model predicts that coupled nephrons having differing gains and TGF delays can produce a variety of complex oscillatory waveforms. The associated power spectra exhibit the signatures of both $1-f$ and $2-f$ frequencies. Both the $1-f$ and $2-f$ signatures may exhibit frequency doublets.
4. The waveforms and power spectra arising in our model of coupled nephrons are similar to complex waveforms and corresponding power spectra from hypertensive rats: $1-f$ and $2-f$ frequencies appear in both model and experimental power spectra. Thus we hypothesize that irregular oscillations in hypertensive rats are attributable, at least in part, to mixed mode $1-f$ and $2-f$ oscillations in coupled nephrons.
5. Power spectra from hypertensive rats contain other frequency signatures that remain to be explained.

References

- [1] Barfred, M., E. Mosekilde, and N.-H. Holstein-Rathlou. Bifurcation analysis of nephron pressure and flow regulation. *Chaos* 6: 280-287, 1996.
- [2] Holstein-Rathlou, N.-H. Synchronization of proximal intratubular pressure oscillations: evidence for interaction between nephrons. *Pfluegers Arch.* 408:438-443, 1987.
- [3] Holstein-Rathlou, N.-H. A closed-loop analysis of the tubuloglomerular feedback mechanism. *Am. J. Physiol.* 261 (*Renal Fluid Electrolyte Physiol.* 30): F880-F889, 1991.
- [4] Holstein-Rathlou, N.-H., and P. P. Leyssac. TGF-mediated oscillations in proximal intratubular pressure: Differences between spontaneously hypertensive rats and Wistar-Kyoto rats. *Acta. Physiol. Scand.* 126: 333-339, 1986.
- [5] Holstein-Rathlou, N.-H., and D. J. Marsh. A dynamic model of the tubuloglomerular feedback mechanism. *Am. J. Physiol.* 258 (*Renal Fluid Electrolyte Physiol.* 27): F1448-F1459, 1990.
- [6] Just, A., U. Wittman, H. Ehmke, and H. R. Kirchheim. Autoregulation of renal blood flow in the conscious dog and the contribution of the tubuloglomerular feedback. *J. Physiol.* 506.1:275-290, 1998.
- [7] Layton, H. E., E. B. Pitman, and L. C. Moore. Bifurcation analysis of TGF-mediated oscillations in SNGFR. *Am. J. Physiol.* 261 (*Renal Fluid Electrolyte Physiol.* 30): F904-F919, 1991.
- [8] Leyssac, P. P., and L. Baumbach. An oscillating intratubular pressure response to alterations in Henle loop flow in the rat kidney. *Acta. Physiol. Scand.* 117: 415-419, 1983.
- [9] Yip, K.-P., N.-H. Holstein Rathlou, and D. J. Marsh. Chaos in blood flow control in genetic and renovascular hypertensive rats. *Am. J. Physiol.* 261 (*Renal Fluid Electrolyte Physiol.* 30): F400-F408, 1991.

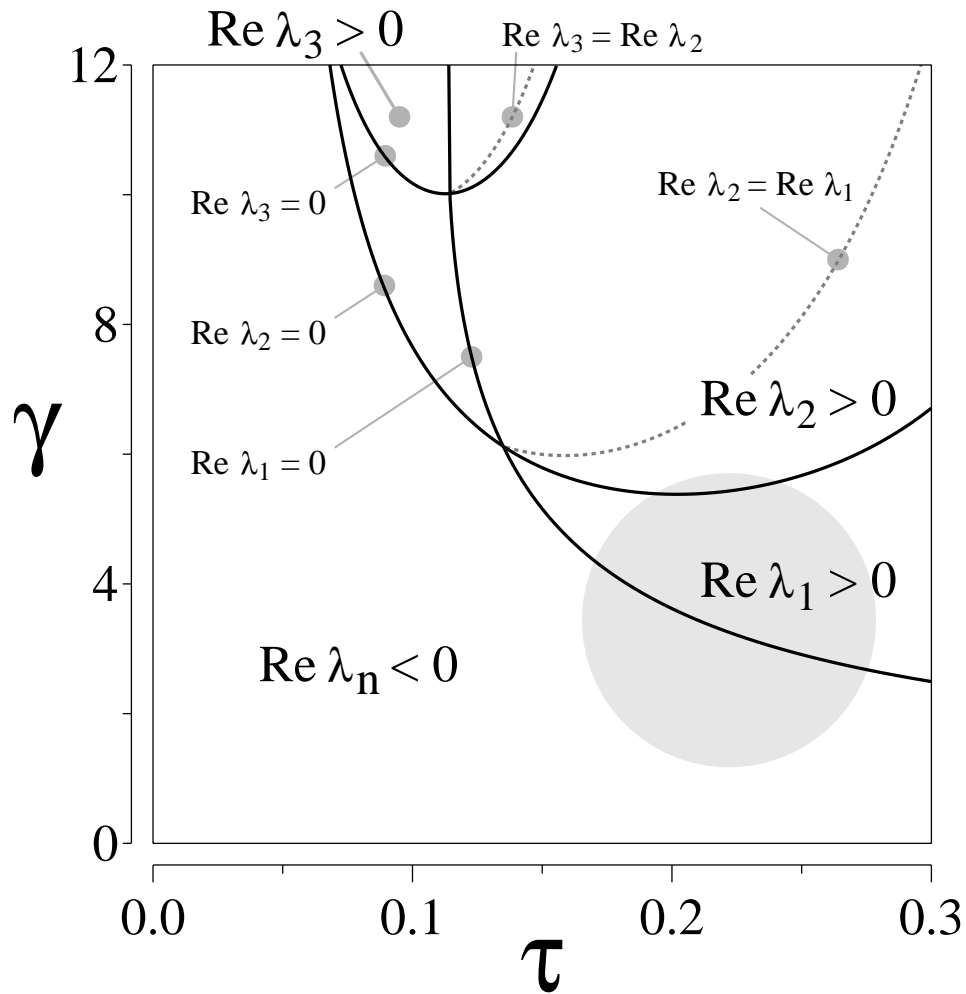


FIGURE M2. Bifurcation diagram based on characteristic equation for linearized model equations. Diagram predicts the steady-state and oscillatory behaviors based on the real (Re) parts of the eigenvalues λ_1 , λ_2 , and λ_3 . Positive real parts indicate potential oscillatory solutions. Confirmation of solution behaviors depends on numerical simulations using the full model equations.

Thus, above the curve $\text{Re } \lambda_1 = 0$, 1- f oscillations are possible; above the curve $\text{Re } \lambda_2 = 0$, 2- f oscillations are possible, especially above $\text{Re } \lambda_2 = \text{Re } \lambda_1$, where $\text{Re } \lambda_2 > \text{Re } \lambda_1$.

This bifurcation diagram is for the base-case parameters (thus with scaling $\zeta = 1$) and is appropriate, we think, for normotensive rats. The normotensive parameter regime for delay τ and gain γ corresponds to the gray disk.

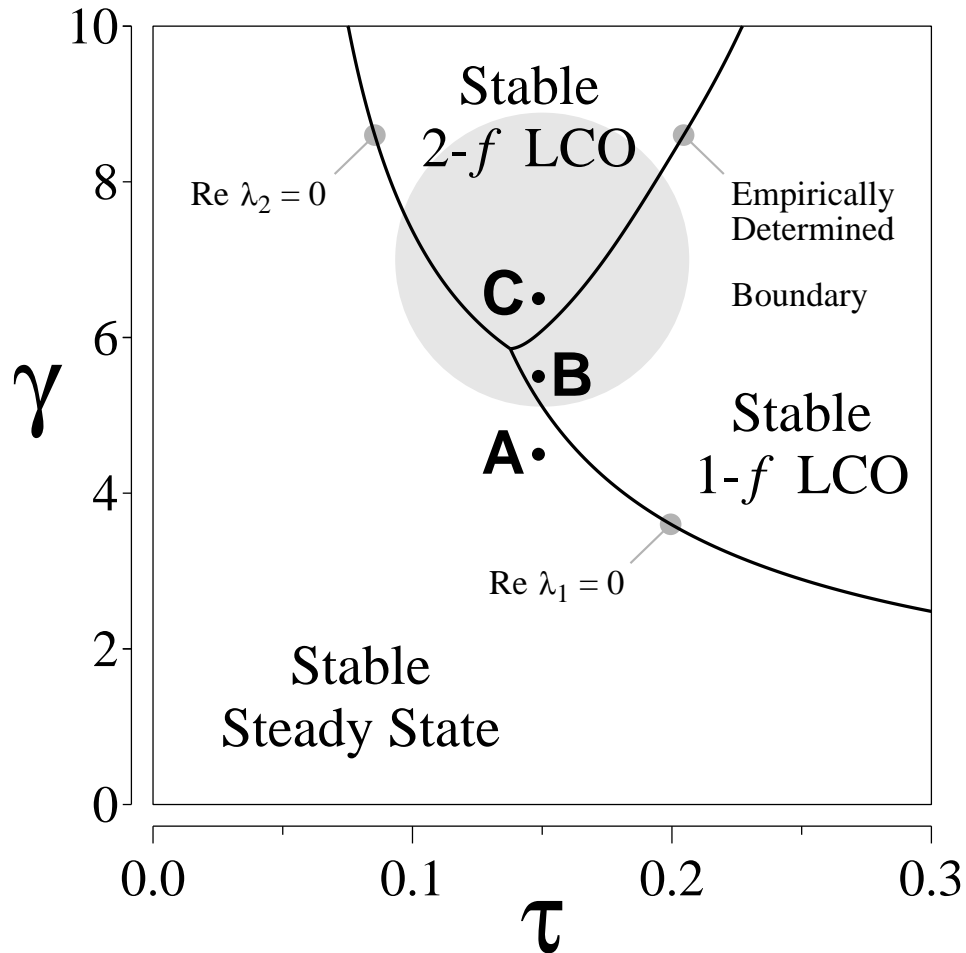


FIGURE 2. Bifurcation diagram for hypertensive rats ($\zeta = 2/3$). In the region labeled “Stable Steady State,” the only stable solution is the time-independent steady state. In region labeled “Stable 2- f LCO” stable oscillations have a frequency about twice that found in region labeled “Stable 1- f LCO.” Gray disk corresponds to the likely parameter range for hypertensive rats. Point **A** corresponds to Fig. 3, Panels A1 and A2; an analogous correspondence holds for Points **B** and **C**.

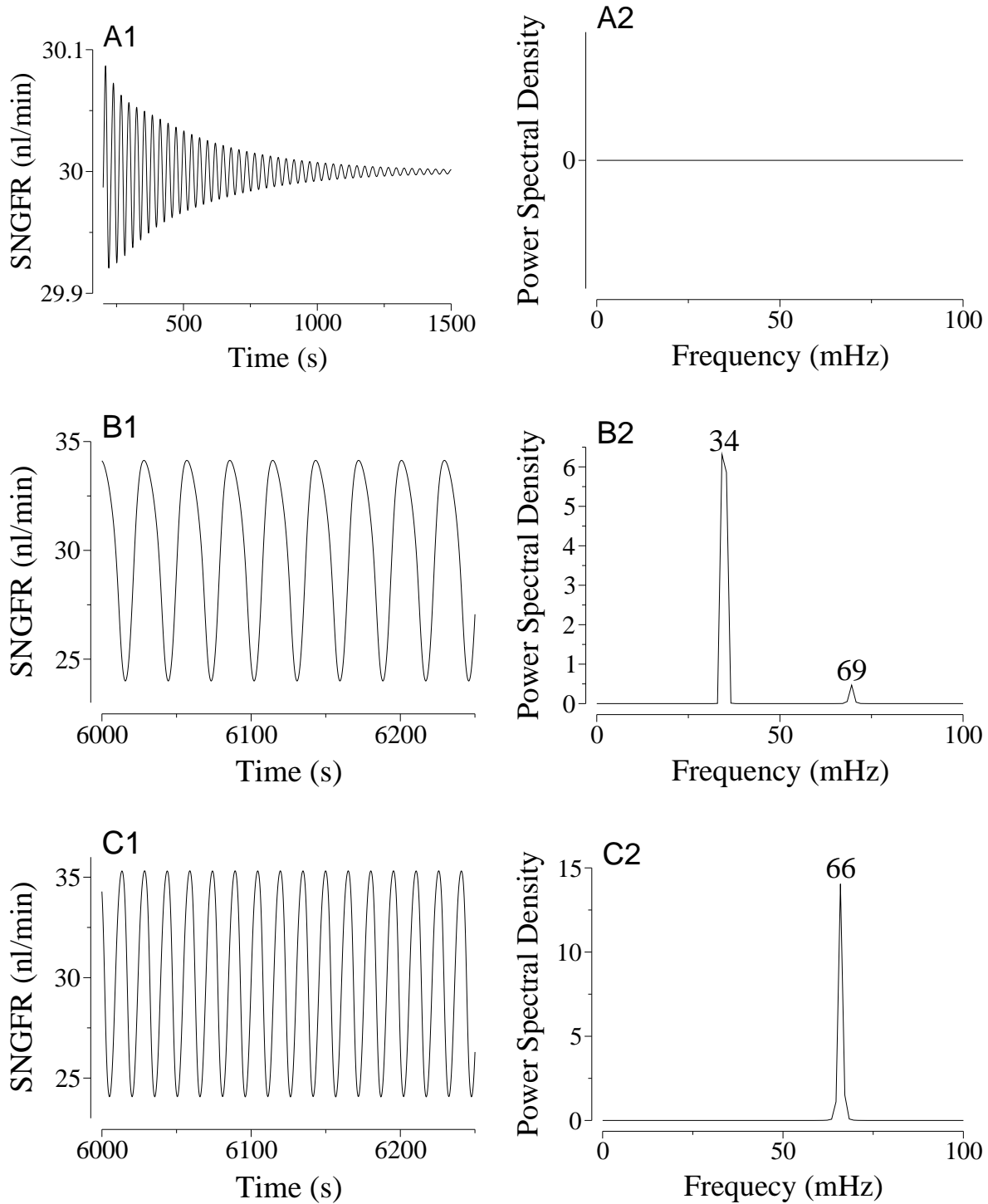


FIGURE 3. Oscillations in SNGFR computed from a mathematical model of a single nephron's TGF system (Panels A1, B1, and C1), and the corresponding power spectra (A2, B2, and C2). Panel A1: return to time-independent steady state after transient perturbation. Panels B1 and C2: stable, sustained oscillations at frequencies $f_1 = 34$ mHz and $f_2 = 66$ mHz, respectively, initiated by a transient perturbation.

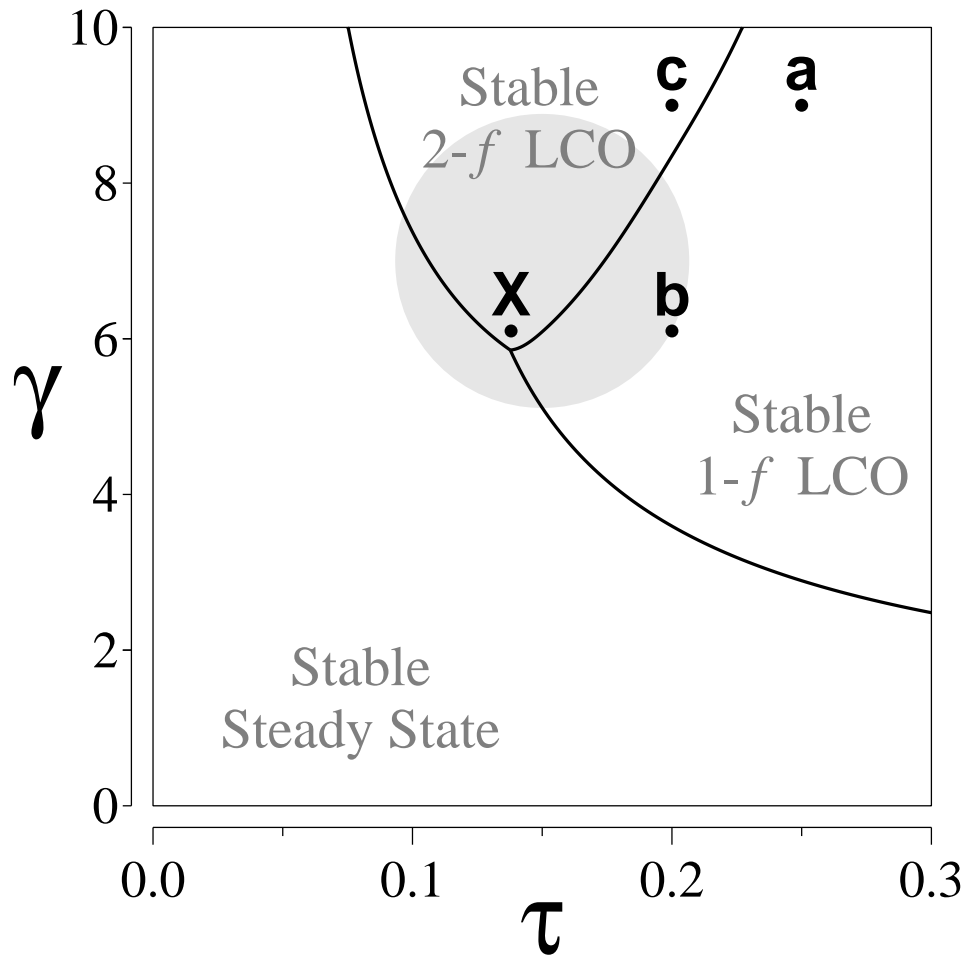


FIGURE 4. Copy of bifurcation diagram for the hypertensive case, from Fig. 2. In a simulation study, TGF systems in two model nephrons were coupled. The system with parameters at Point **X** was coupled with a system with parameters at **a**, **b**, or **c**. The corresponding parameters were

X: $\tau = 0.138, \gamma = 6.1$

a: $\tau = 0.25, \gamma = 9$;

b: $\tau = 0.2, \gamma = 6.1$;

c: $\tau = 0.2, \gamma = 9$.

Model simulation results are shown in Fig. 5.

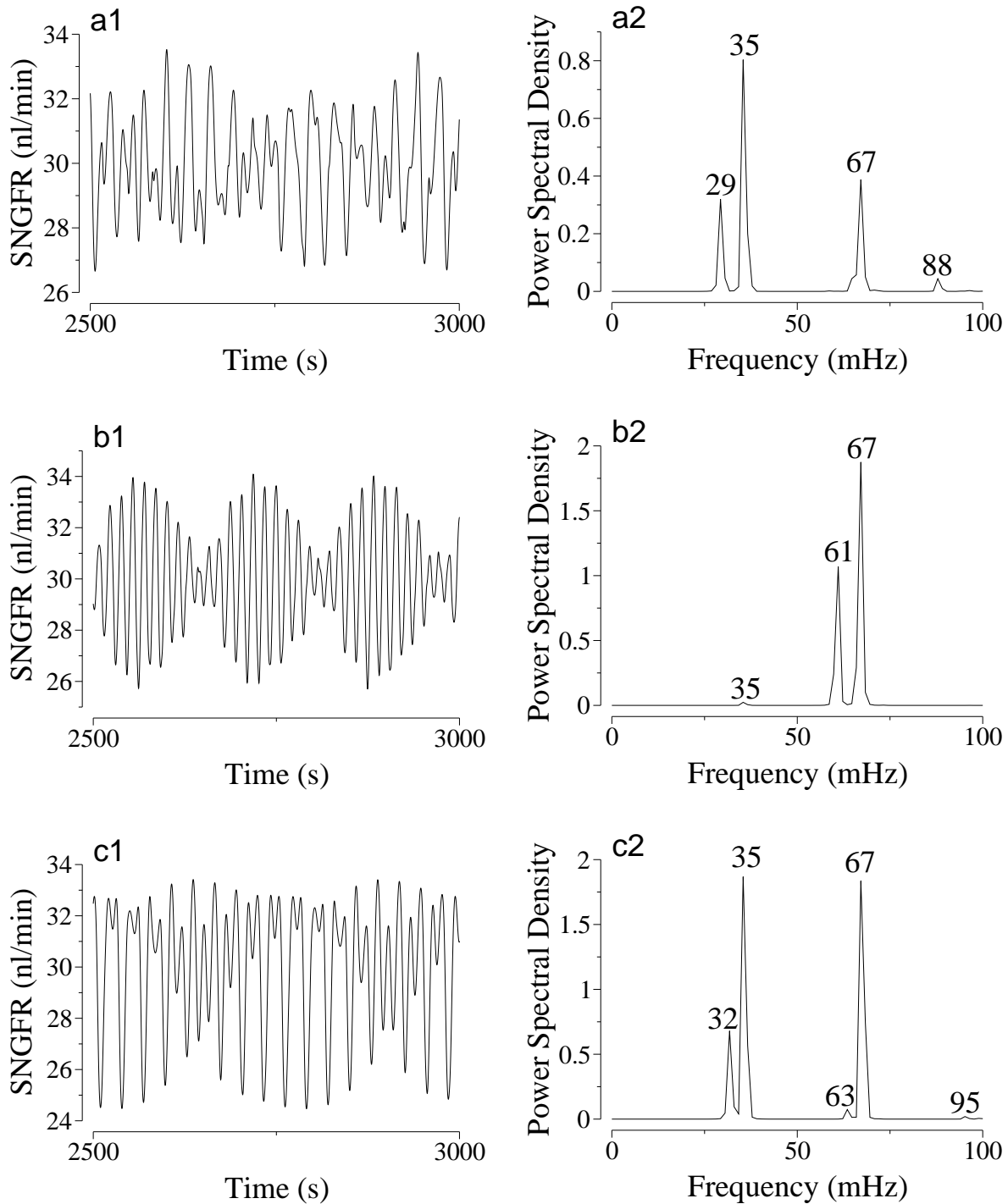


FIGURE 5. Oscillations in coupled-nephron SNGFR simulated by means of the mathematical model: Panel a1 corresponds to parameters indicated by Points **X** and **a**; Panel b1, **X** and **b**; Panel c1, **X** and **c**. Corresponding power spectra are given in Panels a2, b2, and c2.